J. Fluid Mech. (2009), *vol.* 624, *pp.* 281–291.
doi:10.1017/S0022112009005916 Printed in the United Kingdom

A free-surface and blockage correction for tidal turbines

J. I. WHELAN†, J. M. R. GRAHAM AND J. PEIRÓ

Department of Aeronautics, Imperial College London,
South Kensington Campus, London SW7 2AZ, UK

(Received 26 September 2008 and in revised form 8 January 2009)

The effects of free-surface proximity on the flow field around tidal stream turbines are modelled using actuator disc theory. Theoretical results are presented for a blocked configuration of tidal stream turbines such as a linear array that account for the proximity of the free surface and the seabed. The theoretical results are compared to open channel flow experimental results in which the flow field has been simulated using a porous disc and strip. These results are complemented by more detailed measurements of the performance of a model horizontal-axis turbine carried out in a water flume and a wind tunnel. The two sets of experiments represent highly blocked and effectively unblocked cases, respectively. The theoretical model of the effects of free-surface proximity provides a blockage correction for axial induction that can be incorporated in blade element momentum codes. The performance predictions obtained with such a code are in good agreement with the experimental results for C_P and C_T at low tip-speed ratios. The agreement weakens with increasing tip-speed ratio, as the wake of turbine enters a reversed flow state. A correction following the philosophy of Maskell is applied to C_T in this region, which provides a better agreement.

1. Introduction

Theoretical models have been established over many years to predict the performance of unconstrained flows through turbines. These have been based on one-dimensional actuator disc flow theory (Betz 1920) and sectional blade element momentum (BEM) theory (Wilson & Lissaman 1974) and have been applied very successfully to both horizontal- and vertical-axis wind turbines. More recently the same type of devices have been developed to extract energy from tidal streams. In these cases the turbine is subject to shallow-water flow, and the rotor is significantly constrained between the seabed and the free surface. As a result tidal turbines are subject to strong blockage effects which can significantly increase the maximum power that can be extracted from the flow by a single open turbine. Antheaume, Maître & Achard (2008) have simulated various blocked conditions using a Navier–Stokes computation coupled with a source term and have shown increased efficiency. BEM codes have been widely adopted by industry to model the aerodynamic performance and loading of the rotor due to their computational efficiency compared to vortex and computational fluid dynamics (CFD) models; however blockage effects (such as the presence of the ground) are normally ignored. This paper will present a method

† Email address for correspondence: jo.whelan@cantab.net

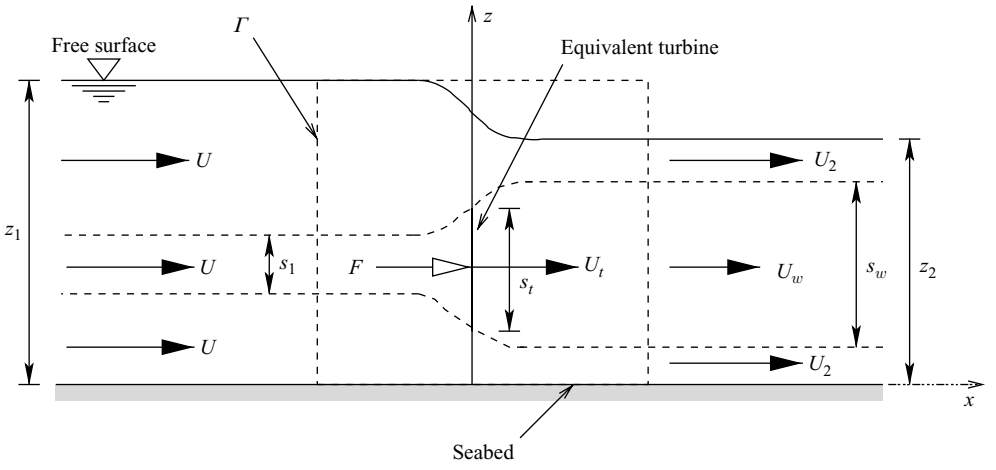

FIGURE 1. Sketch of the two-dimensional approximation to the flow past a tidal turbine.

of evaluating and applying a blockage correction to BEM theory to predict this enhancement.

Garrett & Cummins (2007) have developed a one-dimensional analysis which considers turbine flows constrained between two rigid surfaces. The present paper extends this work to allow for deformation of the free surface due to the pressure changes occurring in the region of the turbine. Deformation of the free surface is associated with a non-zero flow Froude number and may become important when the blockage ratio of the turbine in the relevant flow cross-section is large. Myers & Bahaj (2007) observed a drop in the free surface immediately behind a operating rotor with increasing flow speed. The type of one-dimensional model developed here assumes that changes in the axial velocity of the flow dominate and that crossflow velocities may be neglected in the calculations. Further the model treats the flow field as if it were homogeneous in the transverse direction. The analysis is therefore appropriate for a confined flow such as a transverse array of regularly and relatively closely spaced turbines extending across a channel, strait or estuary. It should also be applicable away from the ends of a large array of turbines in which the width of the turbine array is significantly greater than the depth, provided careful consideration is taken of the upstream flow. Such turbine arrays have been proposed as an efficient means of extracting tidal stream energy with minimum disruptions to the environment (Carbon Trust 2005). The free-surface model developed here is also applicable to any device causing a pressure drop in the flow direction.

2. Modelling free-surface proximity

We consider an infinite array of rotors situated across a tidal stream in water of depth z_1. The theory makes no assumption about the relative vertical height of the turbine as long as it is fully submerged. The seabed is assumed to be horizontal. These rotors will be represented by actuator discs. Where the rotor spacing is fairly close, a first approximation for the effects of free-surface and seabed proximity can be obtained by considering a transversely averaged flow, as shown in figure 1. The area of the 'actuator (or resistance) strip' per unit transverse width of the flow is taken to be equal to the area occupied by rotor discs per unit width; i.e. their blockage ratio

$B = s_t/z_1$ is the same. An infinite array of rotors may be conveniently represented in a laboratory by a single rotor in a rectangular cross-section flume.

Following the notation of figure 1, the tidal stream flows with a constant speed U, and the streamtube containing the actuator strip has far downstream an area s_w and a velocity $U_w = \alpha U$. The flow speed across the disc is $U_t = \beta U$. The velocity outside the streamtube (to be referred to hereafter as the bypass flow) far downstream is denoted by $U_2 = \tau U$. It is a standard assumption for blockage corrections that the bypass flow is uniform.

To predict the free-surface height drop due to the turbines' presence as well as the performance characteristics of the device, we will combine the continuity, Bernoulli and momentum equations to derive a quartic equation in terms of τ.

Applying continuity to the flow which does not pass through the rotor (bypass flow) gives

$$U(z_1 - s_1) = \tau U(z_2 - s_w), \tag{2.1}$$

and then applying continuity to the inside streamtube (flow through the rotor) gives

$$Us_1 = \beta Us_t = \alpha Us_w. \tag{2.2}$$

Rearranging (2.1) and (2.2) leads to

$$\beta = \frac{\alpha}{B(\tau - \alpha)}\left[\tau\left(1 - \frac{\delta z}{z_1}\right) - 1\right], \tag{2.3}$$

where $\delta z = z_1 - z_2$ represents the free-surface height drop. Its value is obtained through the use of Bernoulli's equation along the free surface as

$$\frac{\delta z}{z_1} = \frac{Fr^2}{2}(\tau^2 - 1), \tag{2.4}$$

where $Fr = U/\sqrt{gz_1}$ is the upstream Froude number. Assuming that there are no pressure losses downstream of the actuator, the application of Bernoulli's equation along the central streamline separately upstream and downstream of the turbine gives the pressure drop δp across the actuator. Making a further assumption that this pressure drop is the average pressure drop across the disc, the force F on the turbine is

$$F = s_t \delta p = \rho s_t \left[g\delta z + \frac{1}{2}U^2(1 - \alpha^2)\right], \tag{2.5}$$

where ρ is the density of the fluid and g is acceleration due to gravity.

The force on the turbine can also be obtained by applying balance of momentum to the control volume Γ surrounding the turbine and penetrating the free surface, shown in figure 1. Denoting by p, $\dot{m}$ and V the pressure, mass flow and velocity, respectively, we can write

$$\begin{aligned} F &= \int_0^{z_1} (p_a + \rho g z)\, \mathrm{d}z - \int_0^{z_2} (p_a + \rho g z)\, \mathrm{d}z - p_a(z_1 - z_2) \\ &\quad - \rho(z_2 - s_w)(\tau U)^2 - \rho s_w(\alpha U)^2 + \rho z_1 U^2 \\ &= \frac{1}{2}\rho g(2z_1\delta z - (\delta z)^2) + \rho U^2 z_1(1 - \tau) + \rho\beta U^2 s_t(\tau - \alpha), \end{aligned} \tag{2.6}$$

where p_a is the atmospheric pressure.

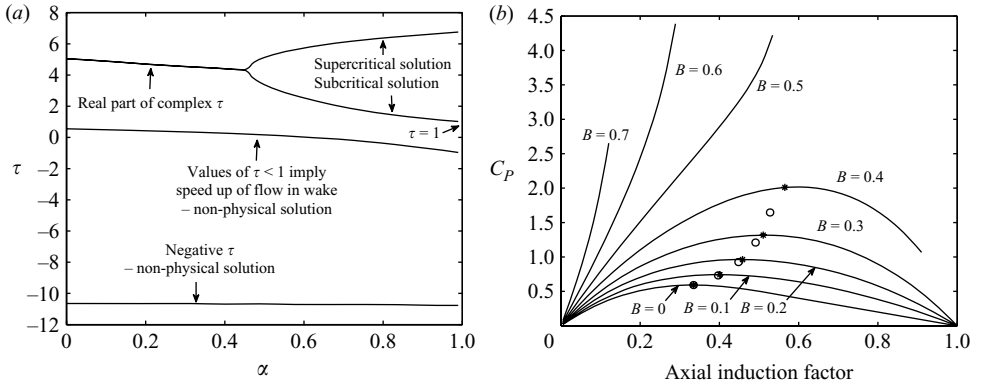

FIGURE 2. (*a*) Method of root selection for the case $Fr = 0.14$ and $B = 0.64$. (*b*) The effect of blockage ratio on power at $Fr = 0.22$: -*- denotes maxima at $Fr = 0.22$; -o- denotes maxima at $Fr = 0$.

Equating (2.5) and (2.6) and substituting for β by (2.3) and $\delta z/z_1$ by (2.4) leads to a quartic polynomial in the change in velocity of the bypass wake flow τ of the form

$$Fr^2\tau^4+4\alpha Fr^2\tau^3+(4B-4-2Fr^2)\tau^2+(8-8\alpha-4Fr^2\alpha)\tau+(8\alpha-4+Fr^2-4\alpha^2B)=0, \quad (2.7)$$

where α is the factor by which the velocity has changed in the far-wake idealization.

This quartic equation yields real solutions for τ for only a subset of inputs for Froude number, blockage ratio and α which correspond to the bypass flow remaining subcritical. An example solution is shown figure 2(*a*). By finding the solution for τ in terms of α, it is then possible to calculate various other parameters.

The most frequently used parameter to represent the velocity loss at the turbine plane (here denoted as β) is the axial induction factor $a = 1 - U_t/U$ which is given by

$$a(\alpha) = 1 - \beta. \quad (2.8)$$

The thrust coefficient is

$$C_T(\alpha) = \frac{F}{\frac{1}{2}\rho U^2 s_t} = (\tau^2 - \alpha^2). \quad (2.9)$$

The power taken out of the flow by the turbine is $P = FU_t$ and the corresponding power coefficient C_P is given by

$$C_P(\alpha) = \frac{P}{\frac{1}{2}\rho U^3 s_t} = \beta(\tau^2 - \alpha^2). \quad (2.10)$$

2.1. *Verification of theory*

As the upstream Froude number falls to zero, the drop in the free surface across the turbine falls to zero. Applying $Fr = 0$ to (2.7) leads to a quadratic polynomial for the change in speed in the bypass wake τ in terms of B and α, which reduces exactly to the case of the solid-wall analysis proposed by Garrett & Cummins (2007),

$$\tau = \frac{1 - \alpha + \sqrt{B - 2\alpha B + \alpha^2(1 - B + B^2)}}{1 - B}. \quad (2.11)$$

Figure 2(*b*) shows the effect of blockage on the variation of C_P with axial induction factor a. In the case in which the blockage ratio decreases to zero, the results from the

free-surface proximity model coincide with the well-known case of an actuator disc in unbounded flow, i.e. the Betz limit, where $C_P = 16/27$. For blockage ratios above 0.3, the lines are discontinued at values of a smaller than 1 due to the supercritical point of wake bypass flow being reached. In such highly blocked cases there is however a significant flow regime in which the bypass flow remains subcritical. Comparison of the maxima at $Fr = 0.22$ with the corresponding values at $Fr = 0$ indicates that C_P increases with both the Froude number and the blockage ratio.

2.2. *Comparison with experiments*

A porous disc is a physical example of an actuator disc often used to simulate a turbine in small-scale laboratory experiments. The pressure drop across a porous gauze or plate is determined by means of a resistance coefficient k as

$$\Delta p = \frac{1}{2} k \rho U_t^2, \tag{2.12}$$

where U_t is the average velocity of the plate (volume flow/area). The axial force on the actuator disc is $F = \Delta p s_t$. Therefore by comparing (2.12) with (2.9) we can then formulate k in terms of the axial induction factor a to give

$$k = \frac{C_T}{(1-a)^2}. \tag{2.13}$$

Experiments were carried out in a water flume with a working section 0.6 m wide, 0.64 m deep and 9 m long. The flume was run at flow speeds up to 0.72 m s^{-1}, corresponding to $Fr = 0.29$ at full depth. A disc with a diameter of 0.4 m was constructed from a porous plate (a solid flat plate drilled with a pattern of holes) in order to provide the required rigidity. The resistance coefficient k of the porous material used was obtained experimentally via force measurements on a piece of the material intersecting the entire flow in the water flume and was found to be approximately 1.8.

The disc in a rectangular duct provides a representation of a turbine in an array ($B = 0.33$). To provide a test of the accuracy of using a one-dimensional theoretical model implying spanwise homogeneity to represent flow about an array of discs, measurements of axial force were also made on a strip 0.6 m $\times$ 0.21 m (i.e. equal blockage to the disc) of the same porous material in the flume.

The force measurements on the disc and the strip agree well with only slight differences at the lowest Froude number and are shown in figure 3. The error in measuring the k of the porous material is estimated to be 10 %. There was an absolute error in measuring C_T which gave a larger relative error at the lowest Froude number. These measurements suggest the two-dimensional analogy is reasonable and are also close to those predicted by the free-surface proximity model. A smaller value of k would lead to a better agreement between measured and predicted results. It can also be seen from figure 3 that the predicted C_T increases with Froude number, although for this range of Froude number, which is likely to be typical for a real tidal turbine, the variation is small.

3. Rotor experiments

Experiments were carried out running the same rotor in two different facilities: the flume described in the previous section (Froude number of 0.14) and a wind tunnel with a cross-section of 1.52 m $\times$ 3.05 m. The rotor has two blades consisting of NACA 6412 aerofoil sections. Each turbine blade is tapered, and the twist decreases

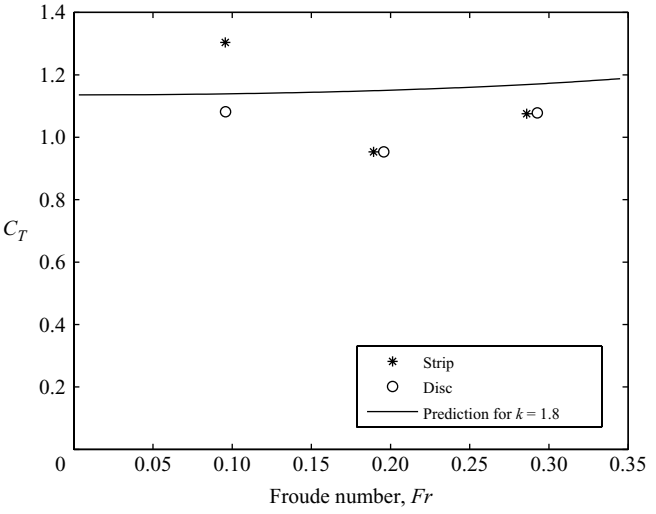

FIGURE 3. Thrust variation with Froude number for $B = 0.33$.

from 33.3° at the root to 5° at the tip. The diameter of the rotor was 0.56 m, leading to blockage ratios of 0.64 in the flume which is a highly blocked case and of 0.05 in the wind tunnel which is effectively unblocked. The results from the experiments carried out in these two facilities will be referred to hereafter as the blocked and unblocked case respectively. The blocked case is almost double the blockage ratio of the porous plate tests. The flow speeds were varied in each facility so that the two Reynolds number ranges were as close as possible. In both cases the Reynolds number at $3r/4$, where r is the radial span position, varied between 7×10^4 and 1.5×10^5. A detailed investigation of the behaviour of the aerofoil section characteristics at this Reynolds number range is given at the end of this section. Measurements of both power and axial force were taken in both tests.

The rotor was suspended vertically downwards from the carriage above the flume and vertically upwards from a point below the floor of the wind tunnel. Power was estimated by measuring torque and rotation speed. The torque was measured using a friction brake arrangement positioned on the downstream side of the rotor. The friction brake consisted of a pulley wheel on the rotor shaft connected to thin strain-gauged cantilever beams via a piece of cord. The torque produced by the rotating turbine was balanced by friction of the cord on the pulley, measured at the cantilever beams. Tightening of the cord enabled control of the rotor speed. The rotation speed ω was measured using an infrared tachometer. In the wind tunnel the turbine rotated at much higher speeds, and it was possible to confirm the measurement from the infrared tachometer using a stroboscope. In both cases measurements of axial force were also taken from strain-gauge measurements of the bending of the supporting strut.

Figure 4 shows the C_P results produced from the experiment carried out on the rotor in both the flume and the wind tunnel. Tip speed ratio Λ is defined as

$$\Lambda = \frac{\omega R}{U}, \tag{3.1}$$

where R is the radius of the turbine. A conservative estimate for tare drag has been taken into account, but no correction has been made for the blockage of the supporting strut because in both cases the facing area of strut exposed to the flow was

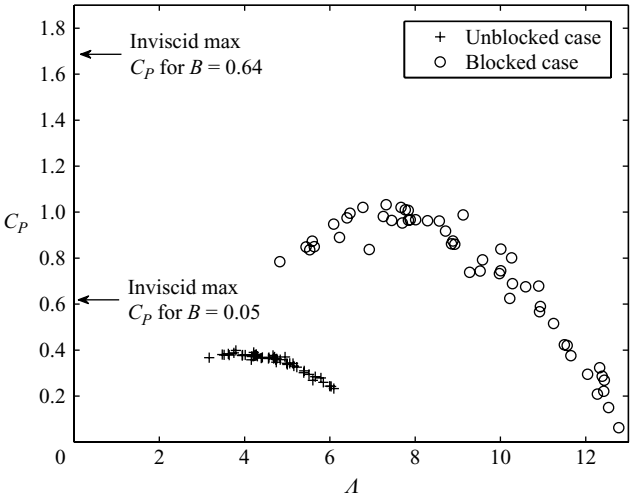

FIGURE 4. Comparison of experimental results and model predictions for C_P versus Λ.

less than 3 % of the rotor swept area. Readings over the whole of the low tip-speed ratio range could not be obtained, since the rotor tended to stall. It can be seen from figure 4 that the values of the performance characteristics measured were much higher in the blocked case than those in the unblocked case. Additionally the readings taken in the flume span a higher tip-speed ratio range. In both cases the ratio between the maximum measured C_P and the maximum inviscid C_P predicted by the free-surface proximity model is approximately 60 %.

3.1. *Aerofoil section characteristics*

A polar curve for the NACA 6412 section was generated by a two-dimensional aerofoil experiment for the blade Reynolds number relevant to the rotor tests. Xfoil (Drela 1989) provides a means of interpolating these results to produce a continuous curve. The blade Reynolds number range of the rotor experiments conducted is moderately low, and therefore the exact transistion point is difficult to predict precisely. In order to validate the results from Xfoil, tests were carried out on a uniform NACA 6412 section (with end plates) connected to a force balance in a wind tunnel facility at Reynolds numbers spanning the range of the rotor tests. Figure 5(*a*) shows the experimental results compared to data generated by Xfoil for a Reynolds number of 10^5. By increasing the drag coefficient as predicted by Xfoil by 30 % it was possible to obtain close agreement with the experimental curve. The requirement for a higher drag coefficient in order to obtain agreement is likely to be due to transition on the aerofoil not being simulated by Xfoil at the position at which it actually occurred. This data was then input to a BEM code, and figure 5(*b*) shows that the predictions agree well with the unblocked tests.

4. Correction for a blade element code

The BEM approach assumes that the force on a blade element can be treated as locally two-dimensional and is related, independently of all other sections, to the momentum change of the fluid that passes through an annulus swept out by that blade element. The effects of viscosity are incorporated into the model empirically through the polar curve of the blade section. The theory for unconstrained flow has

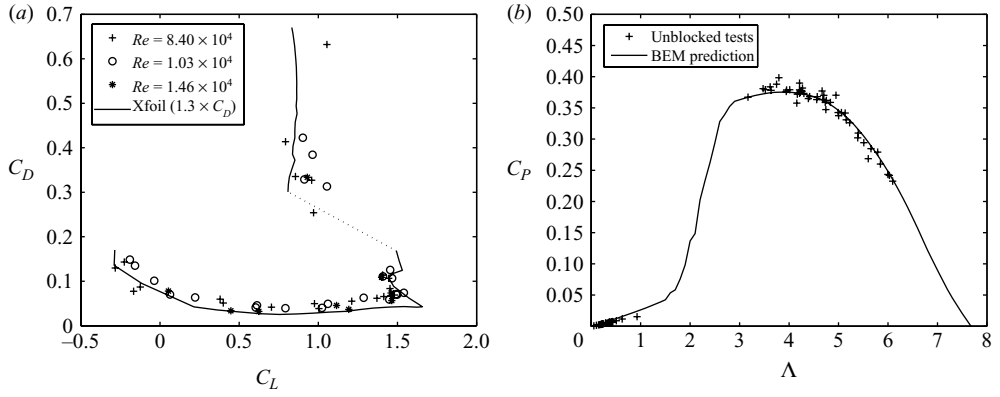

FIGURE 5. (*a*) Polar curve for the NACA 6412 aerofoil section; (*b*) unblocked case experimental results compared to BEM prediction.

been widely documented (e.g. Wilson & Lissaman 1974). Correction procedures for blockage and free-surface proximity in such a code are described here.

4.1. *Application of the correction*

In this work the BEM theory has been implemented using an iteration in which the sectional C_T is obtained initially from the blade forces based on an assumed initial value of angle of attack. The axial induction factor a is then calculated based on this value of C_T, using the free-surface proximity model. Hence a varies depending on the blockage and Froude number, the relationship being obtained by cross-plotting (2.8), (2.9) and the solution to (2.7) and then fitting a curve to the data. Note that when the blockage ratio and Froude number tend to zero, this curve tends to that derived for unconstrained flow obtained by applying mass conservation and Bernoulli, i.e. $C_T = 4a(1-a)$. The effective inflow angle (angle of attack plus blade pitch) is then calculated from the velocity triangle formed from the rotation of the blade (ωr) and the oncoming flow (U) both modified by tangential and axial induction factors respectively. The iteration procedure then uses the new value of angle of attack until convergence of the axial induction factor is achieved within a specified tolerance.

The predictions for C_P and C_T in the highly blocked case are compared to the experimental results in figure 6. The experimental results for C_P and C_T are in reasonable agreement at lower tip-speed ratios. The prediction of the maximum power matches the experimental result. Figure 6 also shows that the effect of Fr is significant at this blockage ratio. The results tend to deviate from the predictions at higher tip-speed ratios. In unconstrained flow at higher tip speed ratios, a reversed flow state occurs in the wake of the turbine (also known as the turbulent wake or brake state). In such an operating state it is not possible to apply Bernoulli's theorem in the wake. An empirical relationship between C_T and a models the behaviour in this regime. Such a relationship is not available for blocked flow. In order to predict or correct the brake state for blockage, a correction for C_T using the philosophy of Maskell (1963) is tried.

4.2. *A correction according to Maskell*

The Maskell theory assumes that the effect of wake and solid blockage is to cause a speed-up in the external flow, and the force coefficients respond as if exposed to that flow. In the present case we assume that the blocked rotor behaves as if exposed to

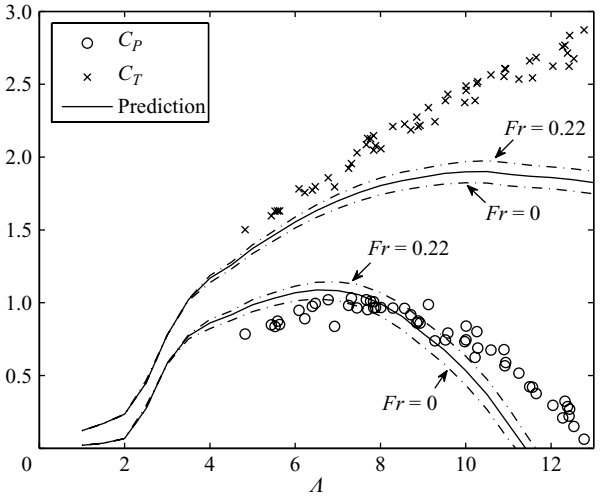

FIGURE 6. Blocked case experimental results compared to BEM predictions; lower set of curves are predictions for C_P; higher set of curves are predictions for C_T.

the bypass blocked flow (τU) as its incident flow. This implies that the Maskell wake blockage factor ϵ is

$$\epsilon = \tau - 1, \tag{4.1}$$

and hence

$$\left[\frac{C_T}{\tau^2}\right]_{(blocked)} = C_{T(unblocked)}. \tag{4.2}$$

The same philosophy would suggest that the tip-speed ratio should be similarly corrected as

$$\left[\frac{\Lambda}{\tau}\right]_{(blocked)} = \Lambda_{(unblocked)}. \tag{4.3}$$

When the measured blocked values of C_T are corrected by this method as for a bluff body in constrained flow there is very good agreement with the unblocked BEM predictions as shown in figure 7. The correction according to Maskell is also shown to be better than the correction proposed by Glauert (1933) for propellers which under-corrects the measured values of C_T. The relationship between the thrust coefficient C_T and the change in velocity of the bypass flow τ is predicted by the free-surface proximity model for the appropriate blockage ratio and Froude number. In order to apply this correction method to permit prediction of rotor thrust in constrained flows by the BEM method it is implemented by using a Newton iteration scheme. The dashed line in figure 7 shows much better agreement with the experimental results at higher tip-speed ratios than the free-surface proximity model prediction.

5. Conclusions

A one-dimensional actuator-disc-type analysis has been developed to incorporate the effects of free-surface proximity and blockage. This theory has been validated by experimental tests using perforated plates and shown to be a good appromixation for the highly blocked flow passed tidal stream turbines in close proximity to the free surface.

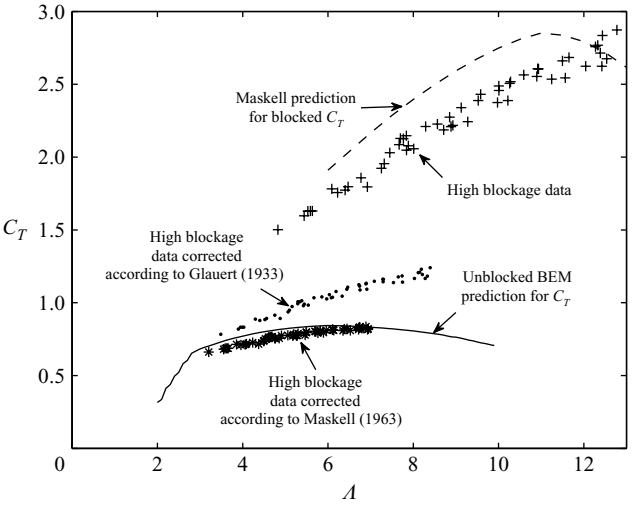

FIGURE 7. Blocked case experimental results corrected to unblocked case according to Maskell.

A correction has been proposed for incorporating the effects of free-surface proximity and blockage into BEM codes routinely used for industrial design of rotors. Performance predictions from both methods have been compared to experimental test results obtained using a model rotor operating under highly blocked conditions in a water flume. The correction directly incorporates the free-surface proximity model into the BEM iteration scheme and has been shown to predict the power and thrust well for low tip-speed ratios. The correction does not work for thrust in the brake state region, and here a prediction according the philosophy of a Maskell correction has been applied which provides better agreement. Further work is required to develop the application of a correction to C_P at high tip-speed ratios and to establish the exact point at which the brake state is effectively turned on. Experimental testing has been restricted to highly blocked cases. However the reasonable agreement achieved between the free-surface proximity model predictions and both sets of tests indicates that the agreement should improve further as blockage is reduced.

We would like to acknowledge the help and support of Mat Thomson from Garrad Hassan and Partners. This work is partly supported by the Engineering and Physical Sciences Research Council through a research studentship.

REFERENCES

ANTHEAUME, S., MAÎTRE, T. & ACHARD, J. 2008 Hydraulic Darrieus turbines efficiency for free fluid flow conditions versus power farm conditions. *J. Renewable Energy* **33**, 2186–2198.

BETZ, A. 1920 Das Maximum der theoretisch möglichen Ausnützung des Windes durch Windmotoren. *Zeitschr. Gesam. Turbinenwesen* **26**, 307–309.

CARBON TRUST 2005 *Variability of UK Marine Resources*. Environmental Change Institute.

DRELA, M. 1989 XFOIL: an analysis and design system for low Reynolds number airfoils. In *Proceedings of the Conference on Low Reynolds Number Aerodynamics*, Nôtre Dame, Indiana.

Garrett, C. & Cummins, P. 2007 The efficiency of a turbine in a tidal channel. *J. Fluid Mech.* **588**, 243–251.

Glauert, H. 1933 Wind tunnel interference on wings, bodies and airscrews. *ARC R&M 1566*.

Maskell, E. 1963 A theory of the blockage effects on bluff bodies and stalled wings in a closed wind tunnel. *ARC R&M 3400.*

Myers, L. & Bahaj, A. S. 2007 Wake studies of a 1/30th scale horizontal axis marine current turbine. *J. Ocean Engng* **34**, 758–762.

Wilson, R. E. & Lissaman, P. B. S. 1974 Applied aerodynamics of wind power machines, Oregon State University.